The STIM-Orai Pathway

2

Structural Insights into Ca^{2+} Sensing by Stromal Interaction Molecules

Peter B. Stathopulos and Mitsuhiko Ikura

2.1 Background

The calcium ion (Ca^{2+}) is a universal messenger which controls a vast number of cellular processes such as the prolonged regulation of transcription, cell division and apoptosis, as well as more short-lived secretion and contraction (Berridge et al. 2000, 2003). The voltage-independent mode of store-dependent Ca^{2+} mobilization is conserved among eukaryotic cells: agonist-induced stimulation of G-protein-coupled or tyrosine kinase receptors activates phospholipase C β or $\gamma 2$, respectively, leading to the hydrolysis of membrane-associated phosphoinositide 4,5-bisphosphate, yielding inositol 1,4,5-trisphosphate (IP_3). IP_3 is a small diffusible second messenger which binds to the IP_3 receptor (IP_3R) on the ER membrane. Binding of IP_3 allosterically opens this Ca^{2+} release channel and Ca^{2+} moves down the concentration gradient from the lumen into the cytoplasm. The endoplasmic reticulum (ER) lumen can only transiently source the cytosol with Ca^{2+} before it is rapidly depleted. In excitable cells, ryanodine receptors (RyRs) play a larger role in sarcoplasmic reticulum (SR) luminal Ca^{2+} depletion than the IP_3Rs. After diminishment of ER/SR stored Ca^{2+}, highly Ca^{2+} selective and permeable store-operated channels (SOC) on the plasma membrane (PM) open, providing sustained Ca^{2+} influx into the cytosol from the virtually inexhaustible extracellular Ca^{2+} supply; ultimately, the cytosolic influx of Ca^{2+} replenishes the luminal stores via the SR/ER

P.B. Stathopulos
Department of Medical Biophysics, Ontario Cancer Institute, University of Toronto, Toronto, ON, Canada

M. Ikura (✉)
Department of Medical Biophysics, Ontario Cancer Institute, University of Toronto, Toronto, ON, Canada

Toronto Medical Discovery Tower, MaRS Centre, Toronto, ON, Canada
e-mail: mikura@uhnres.utoronto.ca

K. Groschner et al. (eds.), *Store-operated Ca^{2+} entry (SOCE) pathways*,
DOI 10.1007/978-3-7091-0962-5_2,

Ca^{2+} ATPase pump. This specific communicative interchange of Ca^{2+} between the ER/SR lumen, cytosol and extracellular space is termed store-operated Ca^{2+} entry (SOCE).

Although the model for SOCE was proposed over two decades ago (Putney 1986), the major molecular players have only been identified and characterized in recent years with the stromal interaction molecules (STIMs) functioning as the ER/SR Ca^{2+} sensors and activators of PM SOCs (Liou et al. 2005; Roos et al. 2005; Zhang et al. 2005), and the Orai proteins serving as the major PM channel components (Feske et al. 2006; Prakriya et al. 2006; Vig et al. 2006a, 2006b; Yeromin et al. 2006; Zhang et al. 2006). Orai1-composed SOCs are termed Ca^{2+} release activated Ca^{2+} (CRAC) channels due to the voltage-independent, highly Ca^{2+} selective and inward-rectifying currents generated during activity, distinct from other SOCs. SOCE via CRAC channels is the primary mode of augmenting cytosolic Ca^{2+} in lymphocyte signaling. Prior to the identification of these molecular components, transient receptor potential (TRP) channels were thought to be major players in CRAC activity (Draber and Draberova 2005; Parekh and Penner 1997; Parekh and Putney 2005; Varga-Szabo et al. 2009).

Human Orai1 is composed of 301 amino acids and has four predicted transmembrane segments (Cai 2007; Feske 2007). Both the amino and carboxy termini of this PM protein reside in the cytoplasm, and each has been implicated as a critical accessory region in Orai1 activation via direct (Ong et al. 2007; Park et al. 2009; Vig et al. 2006a; Yeromin et al. 2006; Yuan et al. 2009) and indirect interactions (Gwack et al. 2007) with STIM1. Glutamate at position 106 in transmembrane segment 1 and Glu190 in transmembrane segment 3 have been identified as key acidic residues for Ca^{2+} ion permeability (Prakriya et al. 2006) and selectivity (Yeromin et al. 2006). Additionally, the Arg91Trp variant associated with inheritable severe combined immunodeficiency (SCID) is located on the first transmembrane segment (Feske et al. 2006). Humans encode three isoforms (i.e. Orai1, Orai2, Orai3) showing conservation in the predicted transmembrane domains, acidic residues involved in ion permeability and selectivity, as well basic residue position associated with SCID. Transmission electron microscopy images of Orai1 used to construct a topology model suggest that Orai1 tetramers form a teardrop-shaped structure that extends into the cytosol sufficiently for direct interaction with STIM1 at ER-PM junctions (i.e. ~10 nm) (Maruyama et al. 2009). Upon ER/SR Ca^{2+} store depletion, STIM1 moves from a pervasive distribution to distinct puncta at ER-PM junctions (Liou et al. 2005; Zhang et al. 2005). This cluster of Ca^{2+} -depleted STIM1 facilitates recruitment of Orai1 to the same junctions, establishing sites of CRAC channel formation (Luik et al. 2006; Varnai et al. 2007; Wu et al. 2006; Xu et al. 2006). For a more comprehensive review on Orai and CRAC channels see Chaps. 3 and 4. The present chapter focuses on the structural, biochemical and biophysical properties of the human STIM1 and STIM2 Ca^{2+} sensing regions critical for the regulation of SOCE and the differences between these isoforms that promote distinct regulatory activity between STIMs.

2.2 Stromal Interaction Molecule Domain Organization

Human STIM1 is a type I transmembrane protein of 685 amino acids localized on ER/SR membranes or on the PM following post-translational glycosylation of Asn131 and Asn171 (Manji et al. 2000; Williams et al. 2001, 2002). Humans encode a second isoform, STIM2, with specific homologous regions to STIM1 within both the luminal and cytosolic domains. Unlike STIM1, STIM2 (i.e. open reading frame of 833 amino acids) does not appear to localize on the PM, despite conservation of the STIM1 Asn131 residue. The most homologous regions between STIM1 and STIM2 include an EF-hand pair, sterile α motif (SAM) domain as well as two cysteines within the luminal domains and three putative coiled-coil domains, a Lys-rich and a Pro/Ser-rich segment within the cytosolic region of the protein (Fig. 2.1a). Both proteins encode a single-pass transmembrane region of 21 amino acids identifiable in bioinformatic hydropathy plots. ER localization of STIM1 is signaled through the first 22 amino acids. STIM2, on the other hand, encodes an additional 87 residues distally toward the N-terminus outside of the homologous ER signal peptide sequences. Early studies suggested that translation initiation of STIM2 occurs at a non-AUG site; however, recently it has been suggested that the much longer signal sequence of STIM2, upstream of and including the homologous STIM1 signal peptide (i.e. residues 1–101) (Fig. 2.1b), is necessary for appropriate ER localization of STIM2 proteins (*vide infra*) (Graham et al. 2011). Phosophorylation of various STIM1 Ser and Thr residues within the Ser/Pro-rich region has been described (Pozo-Guisado et al. 2010; Smyth et al. 2009).

The activation of CRAC by STIM1 is better resolved than STIM2 due to less ambiguous and considerably more cell biology data. The process of CRAC activation by ER/SR-residing STIM1 is a multi-step process: first, STIM1 oligomerization on the ER membrane occurs in response to ER/SR luminal Ca^{2+} depletion; second, STIM1 homotypic oligomers translocate to ER/SR-PM junctions; third, CRAC channels are recruited and open at these junctions (Liou et al. 2007). The cytosolic regions of STIMs play a role in oligomerization of Ca^{2+}-depleted STIM1 (Covington et al. 2010), in targeting the molecule to ER/SR-PM junctions and in interactions with Orai1 pore subunits (Baba et al. 2006; Huang et al. 2006; Li et al. 2007; Liou et al. 2007). Critical regions required for STIM1-Orai1 coupling and CRAC activation have been mapped using live cell experiments. Three separate investigations identified cytosolic STIM1 residues 233–450 (i.e. Orai1 activating small fragment, OASF) (Muik et al. 2009), 342–448 (Park et al. 2009) (i.e. CRAC activating domain, CAD) and 344–443 (Yuan et al. 2009) (i.e. STIM1-Orai1 activating region, SOAR) as critical amino acid stretches through the conserved coiled-coil domains for induction of Orai1 channels. STIM1 likely interacts with both the N- and C-terminal domains of Orai1 in the formation and activation of CRAC channels (see also Chap. 4).

The essential role of STIM1 in the activation of CRAC channels is evident from inhibiting RNA studies which demonstrate a significant attenuation in CRAC entry after STIM1 knockdown (Liou et al. 2007; Roos et al. 2005) and from STIM1/Orai1 co-overexpression data which show very large augmentations in ER Ca^{2+}-depletion

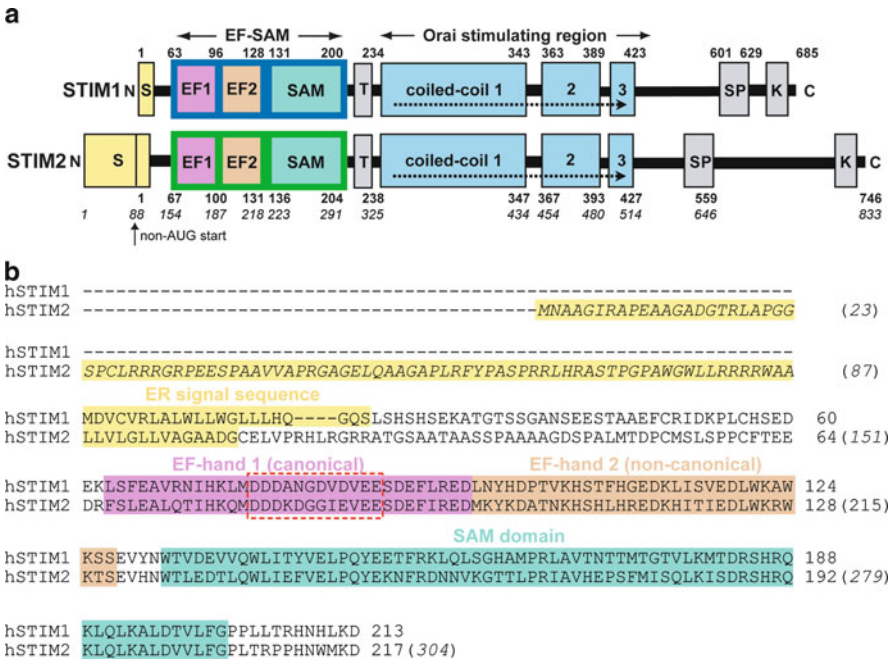

Fig. 2.1 Primary sequence and domain architecture of STIM1 and STIM2. (**a**) Conserved domains in human STIM1 and STIM2. Upstream of the signal peptides, S (*yellow*), the luminal domains include the canonical EF-hand, EF1 (*violet*), the non-canonical EF-hand, EF2 (*beige*), and the SAM domain (*green*). A single transmembrane pass, T, separates the cytosolic portion that include three putative coiled-coil domains (*blue*), a serine/proline-rich region, SP, and a lysine-rich region, K. Residue boundaries are indicated *above* and *below* STIM1 and STIM2, respectively. STIM2 contains a second set of numbering (*italics*) corresponding to the entire STIM2 open reading frame. (**b**) Sequence conservation between human STIM1 and STIM2 luminal regions. Amino acids through the domain boundaries are colored as described in **a**. The canonical EF-hand loop residues involved in Ca^{2+} coordination are bounded by a box (*red, broken lines*). Residues shown in italics are upstream of the non-AUG start site for STIM2. Alignment was performed using ClustalW (Larkin et al. 2007)

dependent SOCE (Mercer et al. 2006; Soboloff et al. 2006). Along with a role in store-operated Ca^{2+} entry, STIM2 more prominently controls basal Ca^{2+} homeostasis (Bird et al. 2009; Brandman et al. 2007). A fraction of STIM2 is coupled to Orai1 at resting ER Ca^{2+} levels, probably due to a somewhat lower affinity for Ca^{2+} (Brandman et al. 2007). Both STIM1 and STIM2 are indispensible in CRAC-induced immune cell activation, even though STIM2 knockout ($^{-/-}$) affects SOCE in T-cells and fibroblasts to a lesser extent than STIM1 ($^{-/-}$) (Bird et al. 2009; Oh-Hora and Rao 2008). Although both isoforms are expressed in a variety of cell types, a vital role for STIM2 has been emphasized in neuronal Ca^{2+} signaling (Berna-Erro et al. 2009). Overall, the present literature suggests that STIM1 is critical for stimulus-induced, SOCE, whereas STIM2 regulates both Ca^{2+}

store-dependent and -independent entry involved with basal Ca^{2+} homeostasis as well as stimulated Ca^{2+} signaling.

The EF-hand and SAM domains located in the luminal region of STIMs are conserved from roundworms to vertebrates (Collins and Meyer 2011; Stathopulos et al. 2009). In humans, the EF-hand together with the SAM domain (i.e. EF-SAM) exhibit greater than 85% sequence similarity (Fig. 2.1b). The conservation of the EF-SAM domain among all phylogeny which express STIM proteins is a testament to the significance of this region in Ca^{2+} signaling by STIMs (Collins and Meyer 2011). Live cell studies demonstrate that EF-SAM provides the machinery necessary to sense changes in luminal Ca^{2+} levels. Specifically, disruption of Ca^{2+}-binding via mutations in the canonical EF-hand causes STIM1 to constitutively form puncta independent of ER Ca^{2+} levels (Liou et al. 2005; Mercer et al. 2006; Roos et al. 2005; Spassova et al. 2006). Furthermore, deleting the SAM domain from STIM1 abrogates the ability of the protein to form inducible puncta (Baba et al. 2006), and exchanging EF-SAM with a rapamycin-inducible oligomerization domain allows control of STIM1 puncta formation via rapamycin treatment, independent of ER Ca^{2+} levels (Luik et al. 2008). Finally, fluorescent protein-tagged STIM1 constructs engineered without the cytosolic domains exhibit very low intermolecular fluorescence resonance energy transfer (FRET) levels at resting ER Ca^{2+} (i.e. consistent with non-interacting EF-SAM domains) that are largely augmented upon Ca^{2+}-store depletion (Covington et al. 2010). In addition to the aforementioned cell biology work, recombinant expression and isolation of STIM1 and STIM2 EF-SAM domains has been a valuable approach in garnering unambiguous biochemical and structural data on this critical sensing region.

2.3 Folding and Ca^{2+} Sensitivity of Isolated EF-SAM Domains

Individual EF-hand and SAM domains have been biochemically and structurally characterized extensively for numerous proteins over the past decades (Ikura 1996; Ikura and Ames 2006; Qiao and Bowie 2005). Throughout nature, EF-hand motifs are found as pairs of helix-loop-helix motifs comprising single domains, and these EF-hand domains are fully capable of folding and cation binding. Similarly, SAM domains have been purified and characterized, folding into compact five-helix bundles, often showing a tendency for intermolecular association. The identification of STIMs as important regulators of CRAC entry inspired the recombinant expression, purification and characterization of these domains, in cis, on the same polypeptide chain, as they occur in STIMs. Remarkably, recombinant STIM1 EF-SAM unfolds through a single, highly cooperative transition using temperature or chemical denaturation (Stathopulos et al. 2006). Similarly, a single and cooperative transition is observed for STIM2 EF-SAM (Zheng et al. 2008), suggesting that the EF-hand and SAM domains of STIMs are co-dependent in overall stability and folding (Fig. 2.2a). The Ca^{2+}-depleted forms (i.e. apo) of STIM1 and STIM2 EF-SAM are markedly less stable than the Ca^{2+}-loaded counterparts (i.e. holo), but also exhibit single, cooperative unfolding curves. The temperature midpoint of

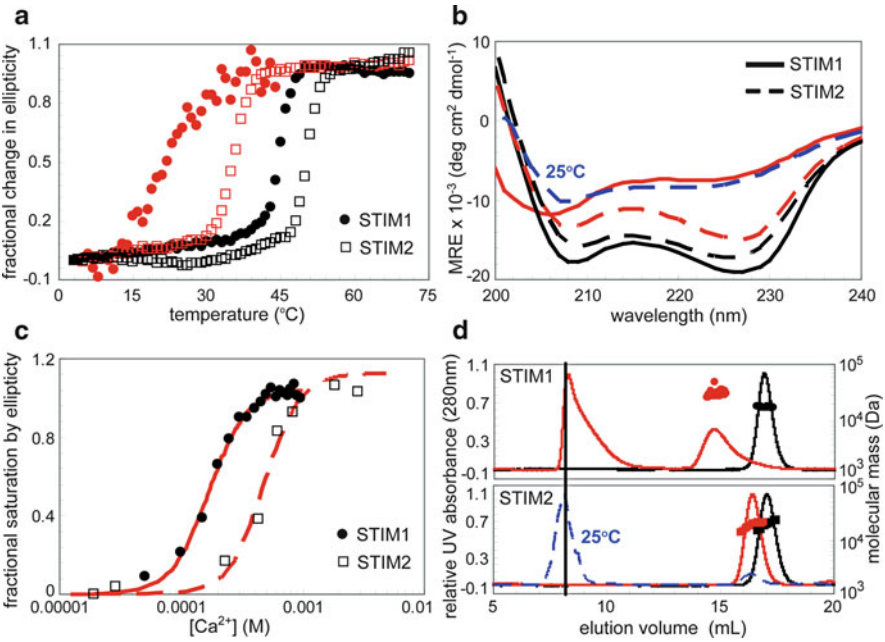

Fig. 2.2 *In vitro* Ca^{2+} sensing characteristics of STIM1 and STIM2 EF-SAM. (**a**) Thermal stability of EF-SAM proteins. The change in far-UV CD at 225 nm is plotted as a function of temperature. Proteins in the presence of excess Ca^{2+} (i.e. holo) are plotted with black symbols and proteins in the absence of Ca^{2+} (i.e. apo) are plotted with red symbols. *Circles* and *squares* represent STIM1 and STIM2 EF-SAM, respectively (Adapted from Stathopulos et al. (2006) and Zheng et al. (2008)). (**b**) Secondary structure of EF-SAM proteins. The far-UV CD spectra of holo and apo STIM1 are shown as solid *black* and *red* lines, respectively. The CD spectra of holo and apo STIM2 are shown as broken *black* and *red* lines, respectively. Apo STIM2 only exhibits a spectrum resembling apo STIM1 EF-SAM at 25°C, shown as a broken *blue* line (Adapted from Stathopulos et al. (2006) and Zheng et al. (2008)). (**c**) Ca^{2+} binding to EF-SAM proteins. Binding to STIM1 EF-SAM monitored by the fractional increase in negative ellipticity at 222 nm is plotted in circles. Binding to STIM2 EF-SAM is plotted in squares. The Hill equation fitted lines are shown in solid and broken *red* lines for STIM1 and STIM2, respectively (Adapted from Zheng et al. (2011)). (**d**) Quaternary structure of EF-SAM proteins. The STIM1 EF-SAM elution profiles in the presence (*black line*) and absence (*red line*) of Ca^{2+} are shown (*upper panel*). The MALS-determined monomeric molecular weight of holo and the dimeric molecular weight of apo STIM1 EF-SAM are shown above the elution peaks. The STIM2 EF-SAM elution profile in the presence (*black line*) and absence (*red line*) of Ca^{2+} is shown (*lower panel*). The MALS-determined monomeric molecular weights for holo and apo STIM2 EF-SAM at 4°C are shown above the corresponding elution peaks. The 25°C elution profile of apo STIM2 EF-SAM is shown as a broken *blue* line. The vertical black line intersects the S200 void volume showing that only apo STIM1 and STIM2 EF-SAM access the oligomerized state (Adapted from Stathopulos et al. (2008) and Zheng et al. (2008))

unfolding (i.e. T_m) in single transition unfolding curves is a good indicator of stability. Apo STIM1 EF-SAM shows a T_m of ~19°C compared to holo STIM1 EF-SAM with a T_m of ~45°C at physiological-like pH (Stathopulos et al. 2006).

The holo and apo states of STIM2 EF-SAM are more stable than STIM1 with T_m values of ~50 and 36°C, respectively (Fig. 2.2a) (Zheng et al. 2008).

The considerable destabilization of STIM EF-SAM domains in response to Ca^{2+}-depletion is the result of a structural allostery. In the case of STIM1 EF-SAM, the protein undergoes a conformational change from a highly α-helical state in the presence of Ca^{2+} to a less well-folded state in the absence of Ca^{2+} (Fig. 2.2b). STIM2 EF-SAM also loses α-helicity in response to Ca^{2+} depletion; however, the structural transition is less striking, with apo STIM2 EF-SAM retaining considerable α-helicity, even in the absence of Ca^{2+} (Fig. 2.2b) (Zheng et al. 2008). The ability of STIM2 EF-SAM to preserve a high degree of α-helicity in the absence of Ca^{2+} is consistent with the lesser destabilization observed in temperature denaturation experiments.

Only one canonical Ca^{2+} binding EF-hand is identifiable in the primary sequence of STIMs (Fig. 2.1b). Consistent with the presence of a single canonical binding loop, STIM1 EF-SAM becomes saturated with Ca^{2+} at a molar ratio of ~1. The equilibrium dissociation constant (i.e. K_d) indirectly calculated using Ca^{2+}-induced changes in tertiary via intrinsic aromatic fluorescence or changes in secondary structure via far-UV circular dichroism, as well as directly measured via $^{45}Ca^{2+}$ titration is high (i.e. K_d between ~0.2 and 0.6 mM) compared to most vertebrate EF-hand proteins (Fig. 2.2c) (Stathopulos et al. 2006). The K_d of Ca^{2+} binding for STIM1 is temperature-dependent, with higher affinities (i.e. lower K_d) at lower temperatures. This temperature trend probably reflects a higher fraction of folded apo STIM1 EF-SAM molecules at lower temperatures. There is a high preference of the EF-hand for Ca^{2+} over Mg^{2+} since inclusion of Mg^{2+} in the experiments does not alter the binding curves. Grafting of the canonically defined EF-hand motif onto a stabilizing CD2 domain, and nuclear magnetic resonance (NMR) titration with Ca^{2+} independently shows a K_d of ~0.5 mM for the STIM1 EF-hand motif in pseudo-isolation (Huang et al. 2009). Considering the high sequence similarity between the STIM1 and STIM2 canonical EF-hand binding loops (Fig. 2.1b), it is not surprising that STIM2 EF-SAM also exhibits a low affinity for Ca^{2+} in the same range as that determined for STIM1 (Fig. 2.2c). Nonetheless, it is important to note that similar probes of Ca^{2+} binding (i.e. fluorescence, CD, $^{45}Ca^{2+}$) applied to the STIM2 EF-SAM system produced considerably higher variability in the curves. This increased error and uncertainty is probably due to a somewhat lower Ca^{2+} affinity, albeit in the same sub-mM K_d range.

The inherent low affinity Ca^{2+} binding EF-hand motifs that STIMs encode are well suited to the relatively high Ca^{2+} levels in the ER/SR lumen. In resting, non-excitable cells the ER luminal Ca^{2+} level is typically between 0.6 and 0.8 mM (Berridge et al. 2000; Berridge et al. 2003). Following agonist-induced stimulation, the luminal Ca^{2+} level may decrease, at least locally, to ~0.2–0.4 mM; moreover, with a Ca^{2+} binding K_d of ~0.2–0.6 mM, STIM1 has evolved to proficiently undergo a shift in the Ca^{2+}-loaded to -free equilibrium in response to these fluctuations in ER Ca^{2+}. The *in vitro* Ca^{2+} binding data for STIM2, at least qualitatively, suggest a decreased affinity compared to STIM1 (Fig. 2.2c).

Consistent with this *in vitro* work, full-length STIM2 forms puncta in response to slighter decreases in ER Ca^{2+} (i.e. at higher ER Ca^{2+} levels) compared to STIM1 (Bird et al. 2009; Brandman et al. 2007). This Ca^{2+} binding property of STIM2 facilitates a role for the ER-localized protein in basal Ca^{2+} homeostasis, since at resting ER Ca^{2+} a significant fraction of STIM2 may be Ca^{2+}-depleted and coupled to Orai1. Contributory to the Ca^{2+} store-independent regulatory mode of STIM2, may be cytosolic STIM2 that is not anchored to the ER membrane (Graham et al. 2011). In the cytosol, the vast majority of STIM2 molecules would be maintained in a Ca^{2+}-depleted state due to the several orders of magnitude lower Ca^{2+} level than the ER lumen (Feske 2007).

2.4 Auto-Inhibition of EF-SAM Oligomerization

Homotypic oligomerization of STIM proteins following ER luminal Ca^{2+} depletion is a decisive initiation step in the activation of SOCE (Liou et al. 2007). In excess Ca^{2+} concentrations, STIM1 EF-SAM strictly exists as a monomer at physiological-like pH and temperatures below the thermal unfolding transition (Fig. 2.2d). In concert with the marked destabilization and partial unfolding accompanying Ca^{2+} depletion, STIM1 EF-SAM undergoes a change in quaternary structure, forming dimers and oligomers at low (i.e. 4°C) and ambient temperatures (Stathopulos et al. 2006). On the other hand, STIM2 EF-SAM exhibits a resistance to oligomerization at low temperature, despite undergoing Ca^{2+}-depletion-induced destabilization, as observed for STIM1 (Fig. 2.2d) (Zheng et al. 2008). At ambient temperature, however, STIM2 EF-SAM oligomerizes, albeit with distinct kinetics compared to STIM1 EF-SAM.

STIM2 EF-SAM exhibits protein concentration dependent oligomerization; higher protein concentrations result in markedly faster oligomerization of apo STIM2 EF-SAM through a concentration range of ~1–10 mg mL^{-1} (Stathopulos et al. 2009). This oligomerized STIM2 EF-SAM is coupled with a partial unfolding event; however, the degree of unfolding, based on far-UV CD spectra is less than that observed for STIM1, even at high protein concentrations (Stathopulos et al. 2009; Zheng et al. 2008). The apo form of STIM1 EF-SAM is persistently dimer-/oligomerized, irrespective of protein concentration. STIM1 EF-SAM, despite the high degree of sequence conservation, has an inherent ability to unfold faster compared to STIM2. This ability is evident in urea-induced unfolding curves which demonstrate single exponential kinetics for both domains, but greater than threefold faster unfolding for STIM1 compared to STIM2 EF-SAM (Stathopulos et al. 2009). The two-state kinetics is in line with the cooperative unfolding of the EF-hand together with the SAM domain and equilibrium denaturation observations. Considering the coupling of partial unfolding to oligomerization, STIM1 EF-SAM is capable of accessing an oligomerization-competent state faster than STIM2 EF-SAM.

2.5 Atomic Three-Dimensional (3D) Structures of Ca^{2+}-Loaded EF-SAM Domains

NMR spectroscopy has been an invaluable tool for teasing out the precise atomic basis for the differences in the physicochemical properties between STIM1 and STIM2 EF-SAM. The Ca^{2+}-loaded form of STIM1 EF-SAM folds into a compact 10-helix structure (Fig. 2.3a, left panel) (Stathopulos et al. 2008). A second EF-hand, not identified in the primary sequence of STIM1, is adjacent to the canonical EF-hand, stabilizing the Ca^{2+}-binding loop through hydrogen bonding. This hydrogen bonding between the canonical and non-canonical EF-hand loops forms a short β-sheet. The 3D structure also exposes a short α-helix, not apparent in the primary sequence, which links the EF-hand pair to the five-helix bundle SAM domain. Overall the majority of the compact structure exhibits an acidic surface charge at neutral pH, particularly concentrated over the EF-hand domain; however, a smaller patch of basic electrostatic potential exists over the SAM domain (Stathopulos et al. 2008).

The NMR structure reveals a basis for the compact nature of STIM1 EF-SAM. Internally within EF-SAM, the EF-hand pair forms a hydrophobic pocket in the Ca^{2+}-loaded state through the side chain orientation of at least 12 amino acids (i.e. Val68, Ile71, His72, Leu74, Met75, Val83, Leu92, Leu96, Lys104, Phe108, Ile115, Leu120) (Fig. 2.3b, left panel). This hydrophobic cleft serves as a dock for non-polar side chains protruding on the distal end of the α10 helix on the SAM domain (i.e. Leu195 and Leu199) (Fig. 2.3a, left panel) (Stathopulos et al. 2008). These intimate hydrophobic contacts between the EF-hand pair and the SAM domain lock STIM1 EF-SAM into a compact fold in the presence of Ca^{2+} which auto-inhibits homotypic association of these domains and keeps STIM1 in a quiescent signaling state. Disruption of the EF-hand:SAM domain interaction via mutation (i.e. Phe108Asp/Gly110Asp or Leu195Arg) facilitates oligomerization of STIM1 EF-SAM *in vitro*, and in live cells within the full-length STIM1 context independent of Ca^{2+} levels. *In vitro*, these EF-hand or SAM mutations cause the protein to adopt an apo-like structure, based on far-UV CD data, but do not alter the Ca^{2+} binding properties of EF-SAM. In live cells, these mutations result in a constitutive puncta formation of STIM1 and activation of SOCs even when the ER luminal Ca^{2+} stores are full (Stathopulos et al. 2008).

As expected from the high sequence conservation between STIM1 and STIM2 EF-SAM, the 3D NMR structure of Ca^{2+}-loaded STIM2 EF-SAM is structurally homologous to STIM1 [i.e. backbone Cα, NH, CO root mean square deviation (rmsd) of 2.7 Å] (Fig. 2.3a, right panel) (Zheng et al. 2011). STIM2 EF-SAM also possesses a second, non-canonical EF-hand motif, suggesting that the EF-hand pair is an important structural feature of all STIMs. In conjunction with the canonical EF-hand, the non-ion-coordinating helix-loop-helix motif forms a hydrophobic pocket, more extensive than that observed for Ca^{2+}-loaded STIM1 EF-SAM. The STIM2 EF-hand non-polar cleft is created by 13 side chains with hydrophobic character (i.e. Leu72, Ile75, His76, Met79, Ile87, Phe95, Met100, Lys103, Lys108, Leu112, Ile119, Leu124, Trp128) (Fig. 2.3b, right panel).

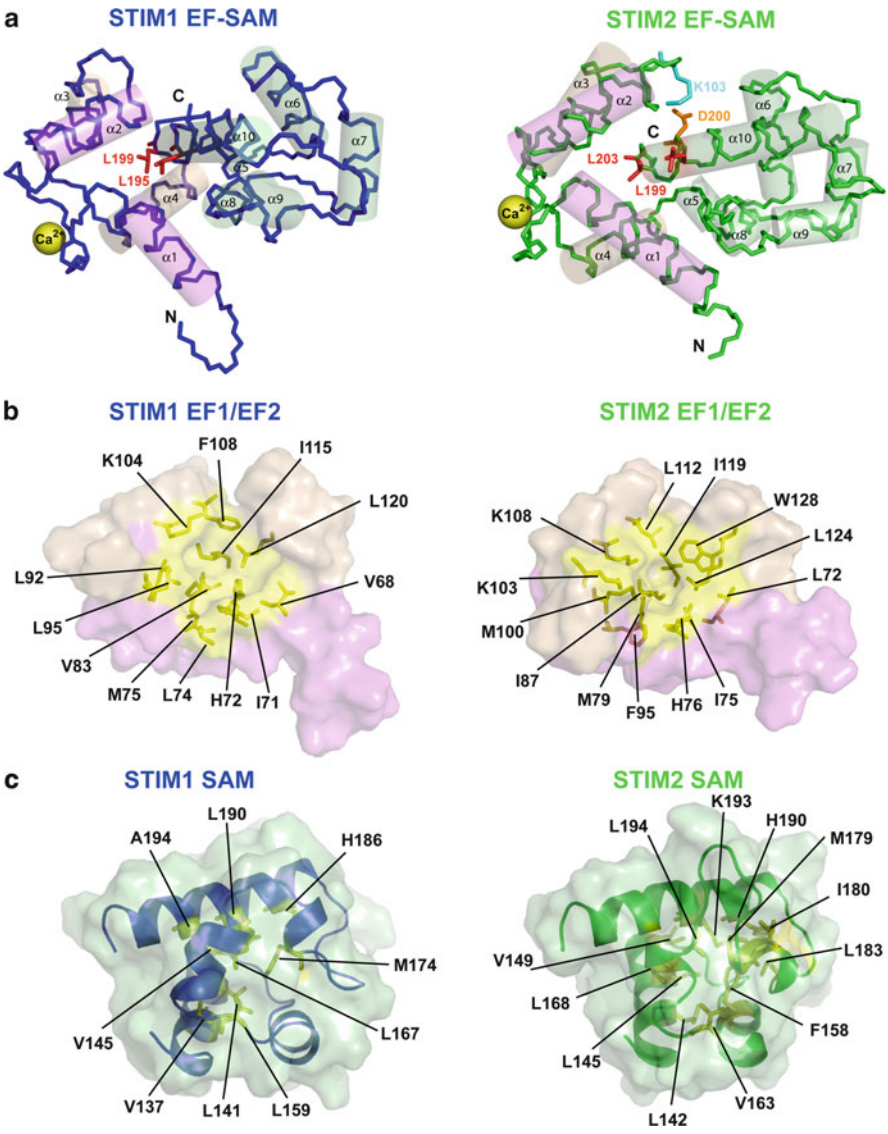

Fig. 2.3 Atomic-resolution NMR structures of STIM1 and STIM2 EF-SAM. (**a**) Structural features of holo EF-SAM proteins. The backbone atoms of Ca^{2+}-loaded STIM1 and STIM2 EF-SAM are traced in *blue* (*left structure*) and *green* (*right structure*), respectively. The canonical EF-hand helices are shown in *violet*, the non-canonical EF-hand helices are in *beige*, and the linker and SAM helices are shown in *green* cylinders. The Ca^{2+} ions coordinated in the canonical loop are shown as *yellow* spheres and the carboxy (C) and amino (N)-termini are indicated. The critical α10 SAM anchor side chains are shown in red sticks. Unique to the STIM2 EF-SAM structure is the complementary positioning of the basic Lys103 (*cyan sticks*) and acidic Asp200 (*orange sticks*) side chains. (**b**) EF-hand cleft architecture of EF-SAM proteins. A surface representation of the EF-hand domains is shown for STIM1 (*left*) and STIM2 (*right*) where coloring is consistent with panel **a**. Residues (*sticks*) and associated surface forming the non-polar clefts are shown as *yellow*.

The Lys103 of STIM2 EF-SAM occurs as an aligned His (i.e. amino acid 99) in STIM1, and the Trp128 occurs as a conserved Trp124 in STIM1; moreover, His99 and Trp124 are directed away from the cleft in the STIM1 EF-SAM structure. The EF-hand domain Lys103 of STIM2 EF-SAM is oriented in close proximity with Asp200 on the α10 helix of the SAM domain, stabilizing the EF-hand:SAM domain interaction via charged interactions (Fig. 2.3a, right panel). The electrostatic surface potential of STIM2 EF-SAM is primarily acidic at neutral pH, with most surface acidic residues clustering in the EF-hand region of the protein (Zheng et al. 2011).

The SAM domain of STIM2 EF-SAM adopts the typical five-helix bundle topology characteristic of these protein-interaction domains (Qiao and Bowie 2005). Twelve residues within the STIM2 SAM domain are greater than 95% inaccessible to solvent (i.e. Leu142, Leu145, Val149, Phe158, Val163, Leu168, Met179, Ile180, Leu183, His190, Lys193, and Leu194) (Fig. 2.3c, right panel). In comparison, STIM1 buries 9 residues within the SAM domain core (Val137, Leu141, Val145, Leu159, Leu167, Met174, His186, Leu190, and Ala194) (Fig. 2.3c, left panel). The hydrophobic STIM2 Ile180 is not conserved in STIM1. This bulky Ile side chain facilitates a rearrangement of residues resulting in the insertion of Phe158 and Lys193 into the STIM2 SAM core (Zheng et al. 2011). These conserved Phe (i.e. amino acid 154) and Lys (i.e. amino acid 189) residues are excluded from the core in STIM1. The STIM2 SAM domain protrusion residues for interaction with the EF-hand pocket include the conserved Leu199 and Leu203 of α10 (Fig. 2.3a, right panel). The enlarged EF-hand hydrophobic cleft, the orientation of basic Lys103 on the EF-hand domain in close proximity to acidic Asp200 on the SAM domain, and the enhanced hydrophobic core of the SAM domain contribute to the augmented stability and attenuated oligomerization propensity observed for STIM2 EF-SAM compared to STIM1 (see above).

2.6 EF-SAM Motif Contribution to STIM Ca^{2+} Sensing

Although composed of separately definable EF-hand and SAM domains, EF-SAMs exhibit a high degree of cooperativity in Ca^{2+}-binding, folding and stability. Despite this mutual dependence, the motifs making up EF-SAM are interchangeable in STIM1/STIM2 chimeras (Zheng et al. 2011). Chimeras designed by swapping the canonical EF-hand, non-canonical EF-hand or the SAM domain encoded by STIM1 and STIM2 provide valuable data on the determinants of distinct sensory

Fig. 2.3 (Continued) (**c**) SAM domain hydrophobic core packing within EF-SAM proteins. The STIM1 and STIM2 SAM backbones are shown as *blue* (*left*) and *green* (*right*) ribbon representations within the SAM domain surface, respectively. Side chains that are greater than 95% inaccessible to solvent are indicated with *yellow sticks*. STIM1 EF-SAM pdbID: 2K60.pdb; STIM2 EF-SAM pdbID: 2L5Y.pdb. Structural images were rendered using PyMol

functions of these proteins. *In vitro*, every combination of STIM1/STIM2 chimeric EF-SAM yields a significant amount of protein with the exception of a combination of the STIM2 canonical EF-hand, STIM2 non-canonical EF-hand and the STIM1 SAM domain (i.e. denoted ES221) (Zheng et al. 2011). All expressible EF-SAM chimeras are sensitive to the presence and absence of Ca^{2+}defined by changes in secondary structure and marked differences in stability. The least stable chimera, aside from the unobtainable ES221, is ES211 while the most stable chimera is ES122. The super-unstable ES211 has apo T_m values ~4 and 19°C lower than wild-type STIM1 and STIM2 EF-SAM, respectively; furthermore, the super-stable ES122 exhibits apo T_m values ~20 and 5°C higher than wild-type STIM1 and STIM2, respectively.

In vitro, the super-unstable ES211 protein is oligomeric, while the super-stable ES122 chimera is monomeric, independent of Ca^{2+} (Zheng et al. 2011). Insertion of these EF-SAM chimeras in place of wild-type within the full-length STIM1 context demonstrates the importance of EF-SAM stability to CRAC regulation. STIM1 with a super-unstable EF-SAM (i.e. ES211), exhibits constitutive puncta in live cells (Fig. 2.4a–c); further, the puncta persistently activate CRAC channels, as the inward rectifying currents generated from Ca^{2+} entry are maximal independent of ER luminal Ca^{2+} levels. On the other hand, STIM1 with a super-stable EF-SAM (i.e. ES122) shows a significant delay in the time to maximal inward rectifying current compared to wild-type STIM1, following passive depletion of ER luminal Ca^{2+} stores (Fig. 2.4a–c) (Zheng et al. 2011). Overall, the chimera observations bring to light two vital characteristics regarding Ca^{2+} sensing by STIMs. First, Ca^{2+} binding affinity endowed by the canonical EF-hand as well as the specific composition of the non-canonical EF-hand and SAM domain are critical contributors to STIM sensory function. Second, nature has selected for STIM isoforms which encode metastable EF-SAM regions that are functionally optimized rather than domains that are stability maximized. By varying EF-SAM stability, STIM1 and STIM2 are able to respond distinctly to similar environmental stimuli.

2.7 Extraneous Luminal Regions Involved in STIM Ca^{2+} Sensing

Considerable primary sequence variability exists within the luminal-oriented regions of STIM1 and STIM2 outside the EF-SAM domains (Fig, 2.1b). These extraneous residues influence Ca^{2+} sensing and regulation of CRAC entry by STIMs. The extension of STIM1 EF-SAM to include all luminal residues outside the signal peptide (i.e. amino acids 23–213) enhances the stability in the presence and absence of Ca^{2+} (Stathopulos et al. 2009). A STIM2 construct engineered with similar aligned boundaries is susceptible to C-terminal degradation; however, a somewhat shorter, degradation-resistant STIM2 protein (i.e. amino acids 15–205)

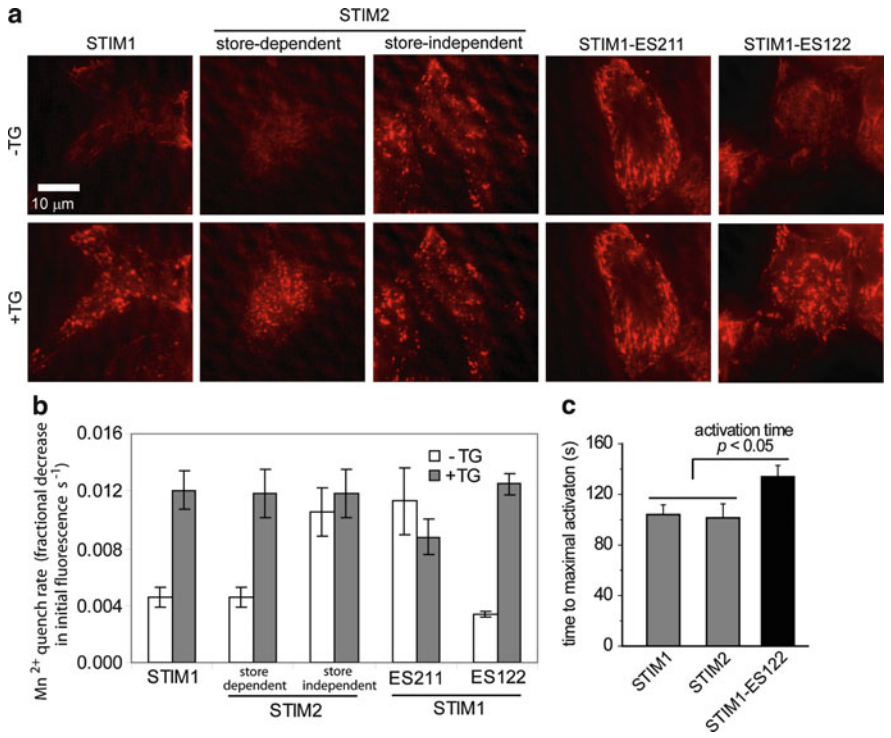

Fig. 2.4 Function of EF-SAM in full-length STIM1 and STIM2. (**a**) Puncta formation by STIM proteins. Total internal reflective fluorescence (TIRF) microscopy shows an ER Ca^{2+} store dependence [i.e. stores must be depleted with thapsigargin (TG)] in the localization of mCherry-STIM1 at ER-PM junctions in HeLa cells. STIM2 exhibits a store-dependent and -independent puncta formation. STIM1 harboring a super-unstable EF-SAM (i.e. ES211) form puncta, independent of ER Ca^{2+} levels, and STIM1 harboring a super-stable EF-SAM (i.e. ES122) exhibit an ER Ca^{2+} dependence in puncta formation similar to wild-type STIM1(Adapted from Zheng et al. (2011)). (**b**) CRAC channel gating by STIM proteins. The Mn^{2+}-induced quench rates of fura-2 loaded into the cytosol of HeLa cells over-expressing STIM proteins are shown. Since CRAC channels are permeable to Mn^{2+} ions the quench rates are an indicator of the open or closed states of Orai1 channels. The quench rates of STIM1 and a fraction of the STIM2 over-expressing cells are significantly increased after treatment with TG. The remaining fraction of STIM2 over-expressing cells show enhanced quench rates independent of ER Ca^{2+} levels (i.e. TG treatment). STIM1 harboring a super-unstable EF-SAM (i.e. ES211) show constitutively open CRAC channels, while proteins harboring the super-stable EF-SAM (i.e. ES122) showed wild-type-like quench rates before and after TG treatment. (**c**) CRAC activation kinetics by STIM proteins. Whole cell inward current density plots of HEK-293 cells co-over-expressing STIM and Orai1 proteins demonstrate that stabilization of the luminal domains via engineering of a super-stable EF-SAM (i.e. ES122) results in an increase in the time to maximal inward current density (i.e. maximal Ca^{2+} influx) (Adapted from Zheng et al. (2011))

also shows an enhanced stability compared to EF-SAM *in vitro*. Far-UV CD data of these extended EF-SAM constructs show less α-helicity per residue in the presence of Ca^{2+} compared to the minimal EF-SAMs, suggesting that the extraneous residues

may have a more prominent affect on the unfolded states of EF-SAM (Stathopulos et al. 2009). In live cells, swapping STIM1 residues 1–65 (i.e. including the STIM1 signal peptide) with STIM2 residues 1–69 and *vice versa* exchanges the CRAC activation phenotype, where full-length STIM1 harboring the STIM2 N-terminal residues exhibits a delay in Orai1 activation and STIM2 fused to the STIM1 N-terminal residues demonstrates wild-type STIM1 CRAC activation kinetics (Zhou et al. 2009).

Two conserved cysteine residues (i.e. Cys49 and Cys56 in STIM1) are encoded in the N-terminal residues extraneous to EF-SAM. Oxidant-induced S-glutathionylation of Cys56 in STIM1 results in constitutive puncta and CRAC entry, suggesting that this Cys residue may afford STIM1 with an additional Ca^{2+}-independent, oxidant-dependent sensory function (Hawkins et al. 2010).

The open reading frame of STIM2 extends 87 residues upstream of the previously determined non-AUG translational start site (Fig. 2.1b) (Williams et al. 2001). Recent data suggests that these 87 upstream residues in addition to the predicted STIM2 ER signal peptide downstream of the non-AUG start site (i.e. residues 88–101; numbering 1–14 downstream of the non-AUG start site) are required for STIM2 to insert into the ER membrane (Graham et al. 2011). With this exceedingly long 101 residue signal peptide, a fraction of STIM2 remains cytosolic, activating PM Orai1 CRAC channels associated with basal Ca^{2+} homeostasis. Interestingly, the 101 amino acid signal peptide that is cleaved from the ER-inserted STIM2 pre-protein may have a function in Ca^{2+}- and SOCE-independent regulation of gene transcription (Graham et al. 2011).

Conclusions

The biochemical, structural and functional data discussed in this chapter delineate four fundamental features contributing to the Ca^{2+} sensing function of EF-SAM domains: (*i*) the binding affinity of the canonical EF-hand, (*ii*) the nature of the EF-hand hydrophobic cleft mutually formed by the canonical and non-canonical EF-hand motifs, (*iii*) the stability of the EF-hand:SAM domain interaction, and (*iv*) the local stability of the SAM domain core. These four elements are not mutually exclusive, but are inter-dependent during Ca^{2+} sensing. Upon Ca^{2+} dissociation from the canonical EF-hand loop, the EF-hand:SAM domain interaction which auto-inhibits oligomerization of this domain is destabilized resulting in partial unfolding-coupled oligomerization. The size of the EF-hand hydrophobic cleft, the complementarity of charged residues between the EF-hand and SAM domains and the local stability of the SAM domain control the extent of destabilization and the distinct oligomerization kinetics observed for STIM proteins. Further structural and biochemical data are required to elucidate the precise mechanism by which luminal residues extraneous to EF-SAM modulate the EF-SAM function.

References

Baba Y, Hayashi K, Fujii Y, Mizushima A, Watarai H, Wakamori M, Numaga T, Mori Y, Iino M, Hikida M, Kurosaki T (2006) Coupling of STIM1 to store-operated Ca^{2+} entry through its constitutive and inducible movement in the endoplasmic reticulum. Proc Natl Acad Sci USA 103:16704–16709

Berna-Erro A, Braun A, Kraft R, Kleinschnitz C, Schuhmann MK, Stegner D, Wultsch T, Eilers J, Meuth SG, Stoll G, Nieswandt B (2009) STIM2 regulates capacitive Ca^{2+} entry in neurons and plays a key role in hypoxic neuronal cell death. Sci Signal 2:ra67

Berridge MJ, Lipp P, Bootman MD (2000) The versatility and universality of calcium signalling. Nat Rev Mol Cell Biol 1:11–21

Berridge MJ, Bootman MD, Roderick HL (2003) Calcium signalling: dynamics, homeostasis and remodelling. Nat Rev Mol Cell Biol 4:517–529

Bird GS, Hwang SY, Smyth JT, Fukushima M, Boyles RR, Putney JW Jr (2009) STIM1 is a calcium sensor specialized for digital signaling. Curr Biol 19:1724–1729

Brandman O, Liou J, Park WS, Meyer T (2007) STIM2 is a feedback regulator that stabilizes basal cytosolic and endoplasmic reticulum Ca^{2+} levels. Cell 131:1327–1339

Cai X (2007) Molecular evolution and structural analysis of the Ca(2+) release-activated Ca(2+) channel subunit, Orai. J Mol Biol 368:1284–1291

Collins SR, Meyer T (2011) Evolutionary origins of STIM1 and STIM2 within ancient Ca(2+) signaling systems. Trends Cell Biol 21:202–211

Covington ED, Wu MM, Lewis RS (2010) Essential role for the CRAC activation domain in store-dependent oligomerization of STIM1. Mol Biol Cell 21:1897–1907

Draber P, Draberova L (2005) Lifting the fog in store-operated Ca2+ entry. Trends Immunol 26:621–624

Feske S (2007) Calcium signalling in lymphocyte activation and disease. Nat Rev Immunol 7:690–702

Feske S, Gwack Y, Prakriya M, Srikanth S, Puppel SH, Tanasa B, Hogan PG, Lewis RS, Daly M, Rao A (2006) A mutation in Orai1 causes immune deficiency by abrogating CRAC channel function. Nature 441:179–185

Graham SJ, Dziadek MA, Johnstone LS (2011) A cytosolic STIM2 pre-protein created by signal peptide inefficiency activates ORAI1 in a store-independent manner. J Biol Chem 286:16174–16185

Gwack Y, Srikanth S, Feske S, Cruz-Guilloty F, Oh-hora M, Neems DS, Hogan PG, Rao A (2007) Biochemical and functional characterization of Orai proteins. J Biol Chem 282:16232–16243

Hawkins BJ, Irrinki KM, Mallilankaraman K, Lien YC, Wang Y, Bhanumathy CD, Subbiah R, Ritchie MF, Soboloff J, Baba Y, Kurosaki T, Joseph SK, Gill DL, Madesh M (2010) S-glutathionylation activates STIM1 and alters mitochondrial homeostasis. J Cell Biol 190:391–405

Huang GN, Zeng W, Kim JY, Yuan JP, Han L, Muallem S, Worley PF (2006) STIM1 carboxyl-terminus activates native SOC, I(crac) and TRPC1 channels. Nat Cell Biol 8:1003–1010

Huang Y, Zhou Y, Wong HC, Chen Y, Wang S, Castiblanco A, Liu A, Yang JJ (2009) A single EF-hand isolated from STIM1 forms dimer in the absence and presence of Ca^{2+}. FEBS J 276:5589–5597

Ikura M (1996) Calcium binding and conformational response in EF-hand proteins. Trends Biochem Sci 21:14–17

Ikura M, Ames JB (2006) Genetic polymorphism and protein conformational plasticity in the calmodulin superfamily: two ways to promote multifunctionality. Proc Natl Acad Sci USA 103:1159–1164

Larkin MA, Blackshields G, Brown NP, Chenna R, McGettigan PA, McWilliam H, Valentin F, Wallace IM, Wilm A, Lopez R, Thompson JD, Gibson TJ, Higgins DG (2007) Clustal W and Clustal X version 2.0. Bioinformatics 23:2947–2948

Li Z, Lu J, Xu P, Xie X, Chen L, Xu T (2007) Mapping the interacting domains of STIM1 and Orai1 in Ca^{2+} release-activated Ca^{2+} channel activation. J Biol Chem 282:29448–29456

Liou J, Kim ML, Heo WD, Jones JT, Myers JW, Ferrell JE Jr, Meyer T (2005) STIM is a Ca^{2+} sensor essential for Ca^{2+}-store-depletion-triggered Ca^{2+} influx. Curr Biol 15:1235–1241

Liou J, Fivaz M, Inoue T, Meyer T (2007) Live-cell imaging reveals sequential oligomerization and local plasma membrane targeting of stromal interaction molecule 1 after Ca^{2+} store depletion. Proc Natl Acad Sci USA 104:9301–9306

Luik RM, Wu MM, Buchanan J, Lewis RS (2006) The elementary unit of store-operated Ca^{2+} entry: local activation of CRAC channels by STIM1 at ER-plasma membrane junctions. J Cell Biol 174:815–825

Luik RM, Wang B, Prakriya M, Wu MM, Lewis RS (2008) Oligomerization of STIM1 couples ER calcium depletion to CRAC channel activation. Nature 454:538–542

Manji SS, Parker NJ, Williams RT, van Stekelenburg L, Pearson RB, Dziadek M, Smith PJ (2000) STIM1: a novel phosphoprotein located at the cell surface. Biochim Biophys Acta 1481:147–155

Maruyama Y, Ogura T, Mio K, Kato K, Kaneko T, Kiyonaka S, Mori Y, Sato C (2009) Tetrameric Orai1 is a teardrop-shaped molecule with a long, tapered cytoplasmic domain. J Biol Chem 284:13676–13685

Mercer JC, Dehaven WI, Smyth JT, Wedel B, Boyles RR, Bird GS, Putney JW Jr (2006) Large store-operated calcium-selective currents due to co-expression of Orai1 or Orai2 with the intracellular calcium sensor, Stim1. J Biol Chem 281:24979–24990

Muik M, Fahrner M, Derler I, Schindl R, Bergsmann J, Frischauf I, Groschner K, Romanin C (2009) A cytosolic homomerization and a modulatory domain within STIM1 C terminus determine coupling to ORAI1 channels. J Biol Chem 284:8421–8426

Oh-Hora M, Rao A (2008) Calcium signaling in lymphocytes. Curr Opin Immunol 20:250–258

Ong HL, Cheng KT, Liu X, Bandyopadhyay BC, Paria BC, Soboloff J, Pani B, Gwack Y, Srikanth S, Singh BB, Gill DL, Ambudkar IS (2007) Dynamic assembly of TRPC1-STIM1-Orai1 ternary complex is involved in store-operated calcium influx. Evidence for similarities in store-operated and calcium release-activated calcium channel components. J Biol Chem 282:9105–9116

Parekh AB, Penner R (1997) Store depletion and calcium influx. Physiol Rev 77:901–930

Parekh AB, Putney JW Jr (2005) Store-operated calcium channels. Physiol Rev 85:757–810

Park CY, Hoover PJ, Mullins FM, Bachhawat P, Covington ED, Raunser S, Walz T, Garcia KC, Dolmetsch RE, Lewis RS (2009) STIM1 clusters and activates CRAC channels via direct binding of a cytosolic domain to Orai1. Cell 136:876–890

Pozo-Guisado E, Campbell DG, Deak M, Alvarez-Barrientos A, Morrice NA, Alvarez IS, Alessi DR, Martin-Romero FJ (2010) Phosphorylation of STIM1 at ERK1/2 target sites modulates store-operated calcium entry. J Cell Sci 123:3084–3093

Prakriya M, Feske S, Gwack Y, Srikanth S, Rao A, Hogan PG (2006) Orai1 is an essential pore subunit of the CRAC channel. Nature 443:230–233

Putney JW Jr (1986) A model for receptor-regulated calcium entry. Cell Calcium 7:1–12

Qiao F, Bowie JU (2005) The many faces of SAM. Sci STKE 2005:re7

Roos J, DiGregorio PJ, Yeromin AV, Ohlsen K, Lioudyno M, Zhang S, Safrina O, Kozak JA, Wagner SL, Cahalan MD, Velicelebi G, Stauderman KA (2005) STIM1, an essential and conserved component of store-operated Ca^{2+} channel function. J Cell Biol 169:435–445

Smyth JT, Petranka JG, Boyles RR, DeHaven WI, Fukushima M, Johnson KL, Williams JG, Putney JW Jr (2009) Phosphorylation of STIM1 underlies suppression of store-operated calcium entry during mitosis. Nat Cell Biol 11:1465–1472

Soboloff J, Spassova MA, Tang XD, Hewavitharana T, Xu W, Gill DL (2006) Orai1 and STIM reconstitute store-operated calcium channel function. J Biol Chem 281:20661–20665

Spassova MA, Soboloff J, He LP, Xu W, Dziadek MA, Gill DL (2006) STIM1 has a plasma membrane role in the activation of store-operated Ca(2+) channels. Proc Natl Acad Sci USA 103:4040–4045

Stathopulos PB, Li GY, Plevin MJ, Ames JB, Ikura M (2006) Stored Ca^{2+} depletion-induced oligomerization of stromal interaction molecule 1 (STIM1) via the EF-SAM region: an initiation mechanism for capacitive Ca2+ entry. J Biol Chem 281:35855–35862

Stathopulos PB, Zheng L, Li GY, Plevin MJ, Ikura M (2008) Structural and mechanistic insights into STIM1-mediated initiation of store-operated calcium entry. Cell 135:110–122

Stathopulos PB, Zheng L, Ikura M (2009) Stromal interaction molecule (STIM) 1 and STIM2 calcium sensing regions exhibit distinct unfolding and oligomerization kinetics. J Biol Chem 284:728–732

Varga-Szabo D, Braun A, Nieswandt B (2009) Calcium signaling in platelets. J Thromb Haemost 7:1057–1066

Varnai P, Toth B, Toth DJ, Hunyady L, Balla T (2007) Visualization and manipulation of plasma membrane-endoplasmic reticulum contact sites indicates the presence of additional molecular components within the STIM1-Orai1 complex. J Biol Chem 282:29678–29690

Vig M, Beck A, Billingsley JM, Lis A, Parvez S, Peinelt C, Koomoa DL, Soboloff J, Gill DL, Fleig A, Kinet JP, Penner R (2006a) CRACM1 multimers form the ion-selective pore of the CRAC channel. Curr Biol 16:2073–2079

Vig M, Peinelt C, Beck A, Koomoa DL, Rabah D, Koblan-Huberson M, Kraft S, Turner H, Fleig A, Penner R, Kinet JP (2006b) CRACM1 is a plasma membrane protein essential for store-operated Ca^{2+} entry. Science 312:1220–1223

Williams RT, Manji SS, Parker NJ, Hancock MS, Van Stekelenburg L, Eid JP, Senior PV, Kazenwadel JS, Shandala T, Saint R, Smith PJ, Dziadek MA (2001) Identification and characterization of the STIM (stromal interaction molecule) gene family: coding for a novel class of transmembrane proteins. Biochem J 357:673–685

Williams RT, Senior PV, Van Stekelenburg L, Layton JE, Smith PJ, Dziadek MA (2002) Stromal interaction molecule 1 (STIM1), a transmembrane protein with growth suppressor activity, contains an extracellular SAM domain modified by N-linked glycosylation. Biochim Biophys Acta 1596:131–137

Wu MM, Buchanan J, Luik RM, Lewis RS (2006) Ca^{2+} store depletion causes STIM1 to accumulate in ER regions closely associated with the plasma membrane. J Cell Biol 174:803–813

Xu P, Lu J, Li Z, Yu X, Chen L, Xu T (2006) Aggregation of STIM1 underneath the plasma membrane induces clustering of Orai1. Biochem Biophys Res Commun 350:969–976

Yeromin AV, Zhang SL, Jiang W, Yu Y, Safrina O, Cahalan MD (2006) Molecular identification of the CRAC channel by altered ion selectivity in a mutant of Orai. Nature 443:226–229

Yuan JP, Zeng W, Dorwart MR, Choi YJ, Worley PF, Muallem S (2009) SOAR and the polybasic STIM1 domains gate and regulate Orai channels. Nat Cell Biol 11:337–343

Zhang SL, Yu Y, Roos J, Kozak JA, Deerinck TJ, Ellisman MH, Stauderman KA, Cahalan MD (2005) STIM1 is a Ca^{2+} sensor that activates CRAC channels and migrates from the Ca^{2+} store to the plasma membrane. Nature 437:902–905

Zhang SL, Yeromin AV, Zhang XH, Yu Y, Safrina O, Penna A, Roos J, Stauderman KA, Cahalan MD (2006) Genome-wide RNAi screen of Ca(2+) influx identifies genes that regulate Ca(2+) release-activated Ca(2+) channel activity. Proc Natl Acad Sci USA 103:9357–9362

Zheng L, Stathopulos PB, Li GY, Ikura M (2008) Biophysical characterization of the EF-hand and SAM domain containing Ca^{2+} sensory region of STIM1 and STIM2. Biochem Biophys Res Commun 369:240–246

Zheng L, Stathopulos PB, Schindl R, Li GY, Romanin C, Ikura M (2011) Auto-inhibitory role of the EF-SAM domain of STIM proteins in store-operated calcium entry. Proc Natl Acad Sci USA 108:1337–1342

Zhou Y, Mancarella S, Wang Y, Yue C, Ritchie M, Gill DL, Soboloff J (2009) The short N-terminal domains of STIM1 and STIM2 control the activation kinetics of Orai1 channels. J Biol Chem 284:19164–19168

http://www.springer.com/978-3-7091-0961-8

Store-operated Ca2+ entry (SOCE) pathways
Emerging signaling concepts in human (patho)physiology
Groschner, K.; Graier, W.; Romanin, C. (Eds.)
2012, XXII, 482 p. With online files/update., Hardcover
ISBN: 978-3-7091-0961-8